

# Nondiffractive feature of $\gamma N \rightarrow \rho^\pm N$ with $\rho$ -meson electromagnetic multipoles

Byung-Geel Yu\*

Research Institute of Basic Science, Korea Aerospace University, Koyang, 412-791, Korea

Kook-Jin Kong†

Photoproduction of charged  $\rho$  on the nucleon is investigated using  $\rho(770) + \pi(140)$  Regge pole exchanges with the  $\rho$ -meson electromagnetic multipoles taken into account. The significance of the Ward identity at the  $\gamma\rho\rho$  vertex is emphasized for current conservation of the process. Given the  $\pi$  exchange with the well-known coupling constants for  $\gamma\pi\rho$  and  $\pi NN$ , the role of the  $\rho$  exchange is analyzed in the  $\gamma p \rightarrow \rho^+ n$  and  $\gamma n \rightarrow \rho^- p$  processes without model-dependences except for magnetic moment  $\mu_{\rho^\pm} = \pm 2.01$  and electric quadrupole moment  $Q_{\rho^\pm} = \pm 0.027 \text{ fm}^2$  taken from theoretical estimates. The nondiffractive feature of both cross sections with the rapid decrease beyond resonance region is reproduced with the dominance of  $\pi$  exchange over the  $\rho$ . Cross sections for differential and density matrix elements are presented to compare to existing data.

PACS numbers: 11.55.Jy 13.40.-f, 13.60.Le, 13.88.+e, 14.40.Be

It is known that photoproductions of charged  $\rho$ ,

$$\gamma + p \rightarrow \rho^+ + n, \quad (1)$$

$$\gamma + n \rightarrow \rho^- + p, \quad (2)$$

proceed via the nondiffractive scattering of  $t$ -channel mesons. Unlike the much studied case of  $\rho^0$  process, however, little has been known about the production mechanism of the charged process, despite the significance of the process giving a clue on our understanding of electromagnetic structure of spin-1 vector meson [1].

A vector meson of spin-1 has the canonical values for magnetic moment  $\mu_\rho = e_\rho/m_\rho$  and electric quadrupole moment  $Q_\rho = -e_\rho/m_\rho^2$  in the limit of a point-like particle. Thus, empirical evidences different from these may signify a nontrivial dynamics of quarks constituting the vector meson [2, 3].

Cross sections for total, differential, and spin density matrix for the process  $\gamma p \rightarrow \rho^+ n$  were measured in the energy range  $E_\gamma = 2.8 \sim 4.8 \text{ GeV}$  by LAMP2 group [4], and at  $E_\gamma = 9.6 \text{ GeV}$  by the Rochester-Cornell collaboration [5]. In the case of  $\gamma n \rightarrow \rho^- p$  process the total and differential cross sections in the range  $E_\gamma = 1 \sim 5 \text{ GeV}$  were extracted from deuteron target by ABBHMM collaboration at DESY [6, 7]. In particular, the data on the latter process show a sharp peak in the cross section,  $\sigma_{max} \approx 7 \mu\text{b}$  at around  $E_\gamma \approx 1.6 \text{ GeV}$  with the steep decrease following beyond resonance region similar to the former process. Hence, both cross sections exhibit a typical of the nondiffractive process where photoproduction of charged  $\rho$  is expected to proceed via the non-resonant meson exchanges. We note that such a rapid decrease of the resonance peak had also been observed in the  $\gamma p \rightarrow \rho^- \Delta^{++}$  [4] as well as  $\gamma p \rightarrow K^* \Lambda$  photoproductions recently measured in the JLab CLAS collaboration [8].

In this work we investigate charged processes  $\gamma p \rightarrow \rho^+ n$  and  $\gamma n \rightarrow \rho^- p$  within the Regge framework for  $\rho + \pi$  exchanges which utilize the Born approximation amplitude for gauge invariance of the  $t$ -channel  $\rho$  exchange. Existing data on the cross sections including density matrix elements are analyzed without fit-parameters, since we have no cutoff masses in the Regge pole exchange. Moreover, as the coupling constants relevant to the  $t$ -channel  $\rho$  and  $\pi$  exchanges are known from the decay width as well as other reaction process, viz., pion photoproduction, the role of  $\rho$  with the electromagnetic multipoles can be clarified without model-dependence.

Previous works on this issue, however, suffered from theoretical limits because of the difficulty in establishing gauge invariance for the exchange of charged  $\rho$  with the  $\gamma\rho\rho$  vertex coupling to charge, magnetic dipole and electric quadrupole moments [1, 9, 10]. We recall that such an on-shell vertex for the  $\gamma\rho\rho$  coupling employed in these works cannot satisfy the Ward identity that should be addressed prior to any sort of prescriptions for current conservation [11, 12].

As depicted in Fig. 1, the divergence of the  $\gamma\rho\rho$  vertex should respect the Ward identity [11],

$$k_\mu \Gamma_{\gamma\rho\rho}^{\mu\nu\alpha}(q, Q) = (D^{-1})^{\nu\alpha}(q) - (D^{-1})^{\nu\alpha}(Q) \quad (3)$$

with respect to the propagator chosen in the unitary gauge,

$$D^{\nu\alpha}(q) = \frac{-g^{\nu\alpha} + q^\nu q^\alpha / m_\rho^2}{q^2 - m_\rho^2} \quad (4)$$

and its inverse

$$(D^{\nu\alpha})^{-1}(q) = (q^2 - m_\rho^2) \left( g^{\nu\alpha} - \frac{q^\nu q^\alpha}{q^2} \right) - m_\rho^2 \frac{q^\nu q^\alpha}{q^2} \quad (5)$$

The identity in the Eq. (3) enables us to derive the

\* bgyu@kau.ac.kr

† kong@kau.ac.kr

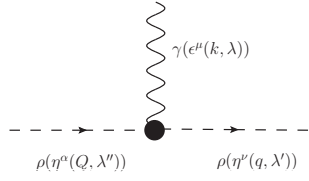


FIG. 1. The  $\gamma\rho\rho$  vertex for the incoming and the outgoing  $\rho$  of momenta and polarizations  $(Q, \lambda'')$  and  $(q, \lambda')$ .

charge coupling term in the  $\Gamma_{\gamma\rho\rho}^{\mu\nu\alpha}$  vertex, i.e.,

$$\begin{aligned}
& e_\rho \eta_\nu^* \Gamma_{\gamma\rho\rho}^{\mu\nu\alpha}(q, Q; k) \eta_\alpha \epsilon_\mu \\
&= -\eta_\nu^*(q) e_\rho \left\{ [(q+Q)^\mu g^{\nu\alpha} - Q^\nu g^{\mu\alpha} - q^\alpha g^{\mu\nu}] \right. \\
&\quad + \kappa_\rho (k^\nu g^{\mu\alpha} - k^\alpha g^{\mu\nu}) - \frac{(\lambda_\rho + \kappa_\rho)}{2m_\rho^2} \left[ (q+Q)^\mu k^\nu k^\alpha \right. \\
&\quad \left. \left. - \frac{1}{2} (q+Q) \cdot k (k^\nu g^{\mu\alpha} + k^\alpha g^{\mu\nu}) \right] \right\} \eta_\alpha(Q) \epsilon_\mu(k) \quad (6)
\end{aligned}$$

which leads to conservation of the production current rather in a simple way similar to the case of pion photoproduction with the contact term. Here  $\epsilon^\mu(k)$  and  $\eta^\nu(q)$  are polarizations of photon and  $\rho$ -meson of momenta  $k$  and  $q$ . The  $\rho$ -meson magnetic moment with the anomalous magnetic moment  $\kappa_\rho$  is taken from Ref. [13], and the electric quadrupole moment  $\lambda_\rho$  is taken to be gauge-invariant for itself from Ref. [12]. For on-shell  $\gamma\rho\rho$  coupling, i.e.,  $\eta^* \cdot q = 0$ , they are reduced to  $\mu_\rho = (1 + \kappa_\rho) \frac{e_\rho}{2m_\rho}$  and  $\mathcal{Q}_\rho = \lambda_\rho \frac{e_\rho}{m_\rho^2}$  with  $\kappa_\rho = 1$  and  $\lambda_\rho = -1$  for a point-like  $\rho$  meson [14], as before. Here we choose  $\kappa_\rho = 1.01$  in favor of the naturalness, and  $\lambda_\rho = -0.41$  in accord with  $\mathcal{Q}_\rho = -0.027 \text{ fm}^2$  [3].

Let us now consider the production amplitude for the  $\gamma N \rightarrow \rho^\pm N$  process based on the diagrams in Fig. 2. In consideration of parity and the decay channels predicted in literature the fully accounted amplitude will consist of the scalar meson  $a_0(980)$ , tensor meson  $a_2(1320)$ , axial mesons  $a_1(1260)$  and  $b_1(1235)$  in addition to  $\rho$  and  $\pi$  exchanges in the  $t$ -channel. For simplicity and clarity of the present issue we here consider the model of  $\rho + \pi$  exchanges, however, because the rest is found to appear in minor role with the contributions of  $10^{-2}$  order at most by the coupling constants predicted from Refs. [15–17], and further from the analysis of Regge-pole fit to data [18].

Then, in order for a fair description of existing data up to  $E_\gamma \simeq 10 \text{ GeV}$  it is natural to take advantage of the  $G$ -parity counting for a determination of the phases of the degenerate trajectories  $\rho$ - $a_2$  and  $\pi$ - $b_1$ , similar to pion photoproduction [15, 19]. For an identification of the sign of the photon-meson coupling it is convenient to define a  $G$ -parity for photon in which case the isoscalar part of the photon has  $G$ -parity negative and the isovector part has  $G$ -parity positive [20]. In diagrams for the  $t$ -channel exchanges in Fig.2,  $G$ -parity negative  $\pi$  and  $G$ -parity positive  $\rho$  couple to the isoscalar photon which

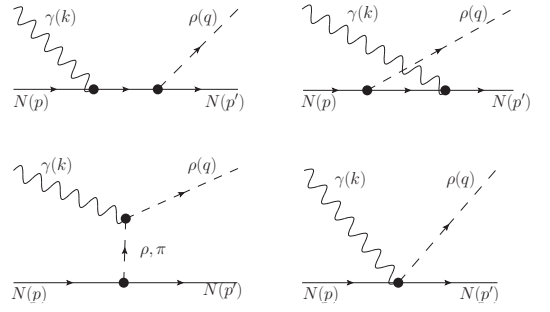


FIG. 2. Feynman diagrams for  $\gamma N \rightarrow \rho^\pm N$ . Nucleon pole terms in  $s$ -, and  $u$ -channel together with the contact term are necessary for gauge invariance of the  $t$ -channel  $\rho$  exchange.

does not change sign in the  $\gamma\pi\rho^\pm$  vertex, whereas  $G$ -parity positive  $b_1$  and  $\rho$  couple to the isovector photon which changes sign in the  $\gamma b_1\rho^\pm$ . Therefore, the signs of the exchange-degenerate (EXD) mesons in the production amplitudes can be written as,

$$\begin{aligned}
\mathcal{M}(\gamma N \rightarrow \rho^\pm N) &\propto (\pm\rho + a_2) + (\pi \pm b_1), \\
&\propto \left\{ \begin{array}{l} \rho e^{-i\pi\alpha_\rho(t)} + \pi e^{-i\pi\alpha_\pi(t)} \\ -\rho(-1) + \pi(1) \end{array} \right\} + \dots, \quad (7)
\end{aligned}$$

where the respective phases are determined according to the addition of each canonical phase,  $\frac{1}{2}((-1)^J + e^{-i\pi\alpha_J(t)})$ . Here the  $\rho$  exchange with the signs denoting the  $\rho$ -meson charge  $e_\rho$  stands for the gauge-invariant amplitude  $\mathcal{M}_{\rho^\pm N}$  as given in Eqs. (12) and (13) below.

In numerical calculations it is found that either the complex or the constant phase for the  $\rho$  exchange will reproduce a slow decrease of the cross section according to the energy-dependence,

$$\sigma \propto s^{\alpha(0)-1}, \quad (8)$$

which is contrary to the rapid slope for the decrease observed in both cross sections. Furthermore, the  $\rho + \pi$  exchanges with the EXD phases in Eq. (7) are largely overestimating both cross sections, unless the intercept of the  $\rho$  trajectory smaller than usual, e.g.  $\alpha_\rho(t) = 0.8t + 0.35$ . For an agreement with experiments, therefore, we assume a violation of the EXD in one of these as in Ref. [18]. Here, we break the EXD of  $\rho$ - $a_2$  to consider the  $\pi$  exchange as the dominant one over the  $\rho$  with the EXD phase in Eq. (7), and assign the canonical phase,  $\frac{1}{2}(-1 + e^{-i\pi\alpha_\rho})$  to  $\rho$  with the trajectories

$$\alpha_\rho(t) = 0.9(t - m_\rho^2) + 1, \quad (9)$$

$$\alpha_\pi(t) = 0.7(t - m_\pi^2), \quad (10)$$

for  $\rho$  and  $\pi$  respectively.

Given the Regge pole,

$$\mathcal{R}^\varphi(s, t) = \frac{\pi \alpha_J'}{\Gamma[\alpha_J(t) + 1 - J] \sin[\pi\alpha_J(t)]} \left( \frac{s}{s_0} \right)^{\alpha_J(t) - J}, \quad (11)$$

written collectively for a meson  $\varphi$  of spin- $J$ , the conserved  $\rho$ -exchange for  $\gamma p \rightarrow \rho^+ n$  is, therefore, given by

$$\begin{aligned} \mathcal{M}_{\rho^+ n} &= \sqrt{2} \bar{u}(p') \eta_\nu^*(q) \left( \Gamma_{\rho p n}^\nu(q) \frac{\not{p}' + \not{k} + M_p}{s - M_\rho^2} \Gamma_{\gamma p p}^\mu(k) \right. \\ &+ e \Gamma_{\gamma \rho \rho}^{\mu\nu\alpha}(q, Q) D_{\alpha\beta}(Q) \Gamma_{\rho p n}^\beta(Q) - e \frac{g_\rho^t}{4M_p} [\gamma^\nu, \gamma^\mu] \left. \right) \epsilon_\mu(k) u(p) \\ &\times (t - m_\rho^2) \times \mathcal{R}^\rho(s, t) \times \frac{1}{2} \left( -1 + e^{-i\pi\alpha_\rho(t)} \right), \end{aligned} \quad (12)$$

and for  $\gamma n \rightarrow \rho^- p$ ,

$$\begin{aligned} \mathcal{M}_{\rho^- p} &= \sqrt{2} \bar{u}(p') \eta_\nu^*(q) \left( \Gamma_{\gamma p p}^\mu(k) \frac{\not{p}' - \not{k} + M_p}{u - M_\rho^2} \Gamma_{\rho p n}^\nu(q) \right. \\ &- e \Gamma_{\gamma \rho \rho}^{\mu\nu\alpha}(q, Q) D_{\alpha\beta}(Q) \Gamma_{\rho n p}^\beta(Q) + e \frac{g_\rho^t}{4M} [\gamma^\nu, \gamma^\mu] \left. \right) \epsilon_\mu(k) u(p) \\ &\times (t - m_\rho^2) \times \mathcal{R}^\rho(s, t) \times \frac{1}{2} \left( -1 + e^{-i\pi\alpha_\rho(t)} \right), \end{aligned} \quad (13)$$

respectively. The coupling vertices  $\gamma NN$  and  $\rho NN$  are given by

$$\Gamma_{\rho NN}^\nu(q) = g_\rho^v \gamma^\nu + \frac{g_\rho^t}{4M} [\gamma^\nu, \not{q}], \quad (14)$$

$$\Gamma_{\gamma p p}^\mu(k) = e \gamma^\mu - \frac{e \kappa_p}{4M} [\gamma^\mu, \not{k}], \quad (15)$$

where  $g_\rho^v=2.6$  and  $g_\rho^t=9.62$  are taken from the vector dominance with the ratio  $g_\rho^t/g_\rho^v = 3.7$  consistent with nucleon anomalous magnetic moment. In the reggeization, we introduce the nucleon pole term for gauge invariance of the  $t$ -channel vector meson exchange. On account of the significance of the magnetic interaction of spin-1 particle we preserve the nucleon magnetic moment  $\kappa_p = 1.79$  in the  $s$ -channel for the process  $\gamma p \rightarrow \rho^+ n$ , and in the  $u$ -channel proton pole term for  $\gamma n \rightarrow \rho^- p$ , respectively.

For the  $\pi$  exchange we write the Regge-pole amplitude as

$$\begin{aligned} \mathcal{M}_{\pi^\pm} &= i\sqrt{2} \frac{g_{\gamma\pi\rho}}{m_0} g_{\pi NN} \varepsilon^{\mu\nu\alpha\beta} \epsilon_\mu \eta_\nu^* k_\alpha q_\beta \bar{u}(p') \gamma_5 u(p) \\ &\times \mathcal{R}^\pi(s, t) \times \begin{Bmatrix} e^{-i\pi\alpha_\pi(t)} \\ 1 \end{Bmatrix}, \end{aligned} \quad (16)$$

for  $\gamma p \rightarrow \rho^+ n$  (upper), and  $\gamma n \rightarrow \rho^- p$  (lower) with  $g_{\pi NN} = 13.4$  and the mass parameter  $m_0 = 1 \text{ GeV}^{-1}$ . Then the coupling constant  $|g_{\gamma\pi\rho}| = 0.224$  is estimated from the width  $\Gamma_{\rho^\pm \rightarrow \pi\gamma} = 68 \text{ keV}$ , and we take the sign of the  $\pi$  contribution with  $\gamma\pi\rho$  coupling relative to  $\rho$  to be more consistent with existing data on both processes.

Fig. 3 shows the dependence of total cross sections upon the sign of  $g_{\gamma\pi\rho}$  coupling constant for  $\rho^+$  and for  $\rho^-$  processes, respectively. We recall that charge asymmetry of the charged  $\rho$  photoproduction off deuteron target is measured in Ref. [5] to be,

$$\frac{\sigma_{\gamma d \rightarrow \rho^+ m} - \sigma_{\gamma d \rightarrow \rho^- m}}{\sigma_{\gamma d \rightarrow \rho^+ m} + \sigma_{\gamma d \rightarrow \rho^- m}} \approx -0.11 \pm 0.03, \quad (17)$$

on the average of the invariant mass  $M_{\pi^+\pi^-}$  interval. From this we could figure out the ratio

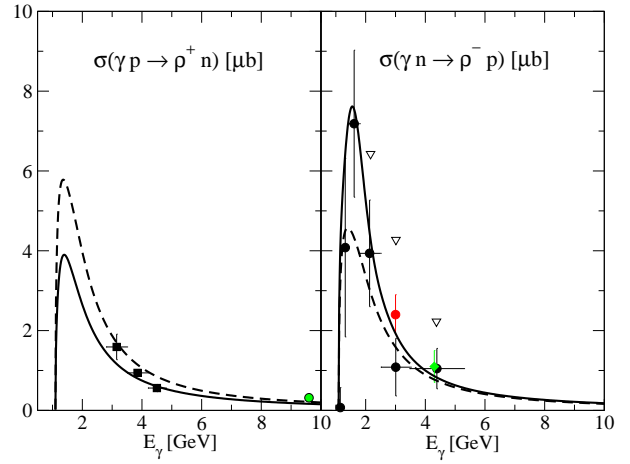


FIG. 3. Dependence of total cross section upon the sign of the  $\gamma\pi\rho$  coupling for  $\rho^+$  (left) and  $\rho^-$  (right) processes. Solid lines result from  $g_{\gamma\pi\rho} = -0.224$  taken for  $\pi$  exchange plus the  $\rho$  exchange with  $\kappa_\rho = 1.01$  and  $\lambda_\rho = -0.41$ . Dashed lines are from the case of  $g_{\gamma\pi\rho} = +0.224$ . Data are taken from Refs

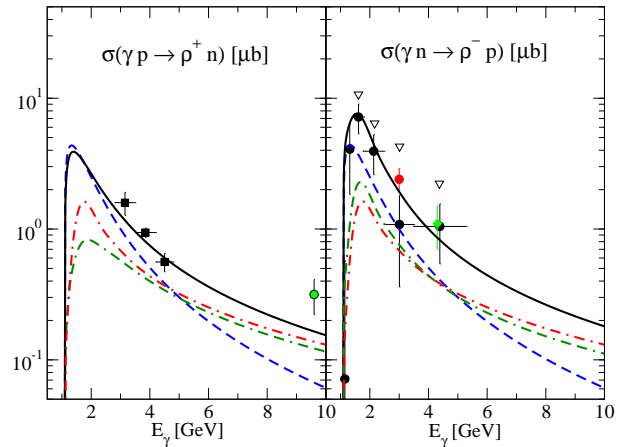


FIG. 4. Contributions of  $\rho$  and  $\pi$  exchanges to total cross section for  $\rho^+$  and for  $\rho^-$  processes. The dashed line (blue) results from  $\pi$  exchange, and the dash-dotted line (red) is from the single  $\rho$  exchange. The dash-dash-dotted line (green) is from the gauge-invariant  $\rho$  exchange,  $\mathcal{M}_{\rho^\pm N}$ .

$\sigma_{\gamma d \rightarrow \rho^- m} / \sigma_{\gamma d \rightarrow \rho^+ m} \approx 1.25$  to expect that  $\sigma_{\rho^-}$  be larger than  $\sigma_{\rho^+}$  in Fig. 3. This is true for the ratio of the total cross sections between  $\pi^+$  and  $\pi^-$  processes which have the same isospin structure with  $\rho^+$  and  $\rho^-$  processes. Thus, the case of the  $g_{\gamma\pi\rho}$  positive is discarded.

In Fig. 4 contributions of  $\rho$  and  $\pi$  exchanges are shown. The dominance of the latter exchange before  $E_\gamma \simeq 5 \text{ GeV}$  in both processes is responsible for the steep decrease of both cross sections. As shown, the different contributions between  $|\rho - \pi|^2$  ( $\rho$  means the  $\mathcal{M}_{\rho^\pm N}$  in green line) for  $\rho^+$  and  $|\rho - \pi|^2$  for  $\rho^-$  productions by the negative coupling  $\gamma\pi\rho$  can help understanding the relative size between the cross sections in this region. Above  $E_\gamma \simeq 5 \text{ GeV}$  the

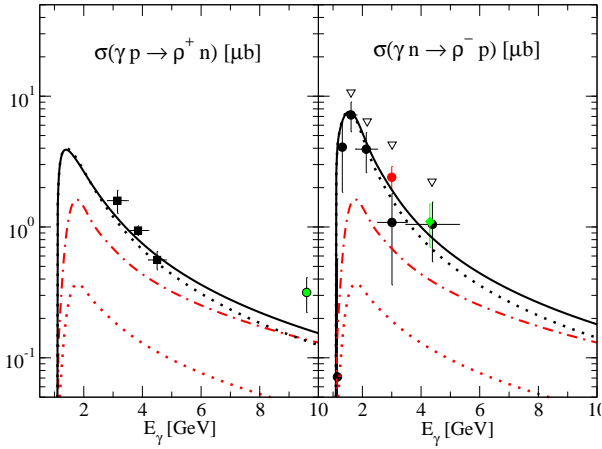


FIG. 5. Dependence of total cross section upon the electromagnetic multipoles of  $\rho$ -meson. The red dotted line rests from the single  $\rho$  exchange with  $\kappa_\rho = 0$  and  $\lambda_\rho = 0$ . The black dotted line is the resultant  $\sigma$  for  $\rho^+$  process (left) and

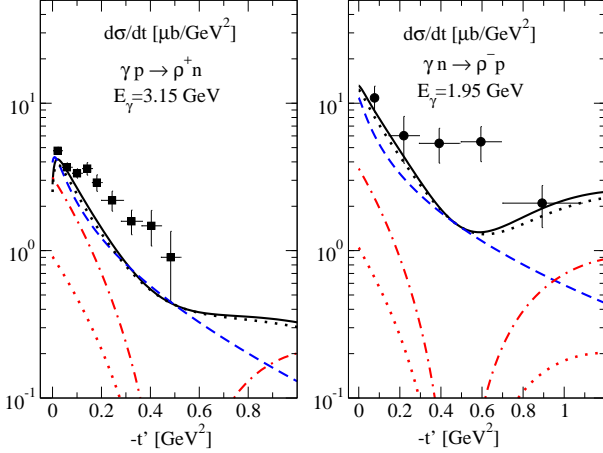


FIG. 6. Contributions of  $\pi$  and  $\rho$  exchanges to differential cross section for  $\rho^+$  at  $E_\gamma = 3.15$  GeV and for  $\rho^-$  at  $E_\gamma = 1.95$  GeV. Notations are the same as Figs. 4 and 5. Data are taken from Refs. [4, 7].

contribution of  $\rho$  exchange becomes dominant over that of  $\pi$  as analyzed in experimental data at  $E_\gamma = 9.6$  GeV [5].

The role of electromagnetic multipoles of  $\rho$  exchange is investigated in Fig. 5 to show the contributions of  $\kappa_\rho$  and  $\lambda_\rho$  to the cross section. The single  $\rho$  exchange (meaning the  $t$ -channel exchange in Fig. 2) with and without them makes itself different by an order of magnitude as shown in the dash-dotted and dotted lines. The role of  $\kappa_\rho$  is found to be more significant than  $\lambda_\rho$ .

Differential cross sections for  $\rho^+$  and  $\rho^-$  processes are presented in Fig. 6 to exhibit a dip structure of  $\rho$  exchange at  $-t \approx 0.5$  GeV<sup>2</sup>/c<sup>2</sup> due to the nonsense-wrong-signature-zero of  $\rho$  trajectory, i.e.,  $\alpha_\rho(t) = 0$ , from the canonical phase. Such a feature raises up the angular

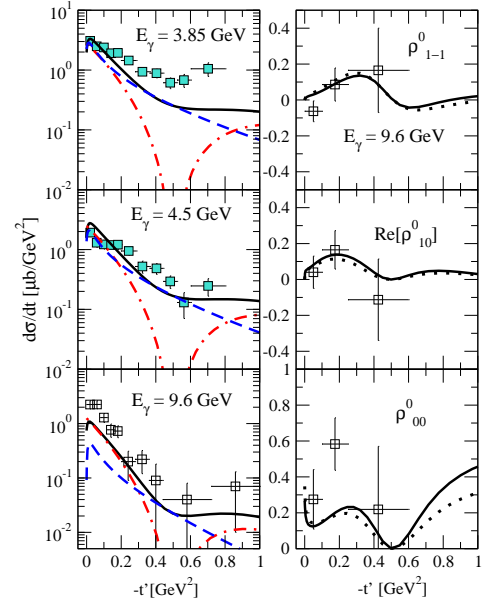


FIG. 7. Differential cross sections in three energy bins and density matrix elements  $\rho_{\lambda\lambda'}^0$  at  $E_\gamma = 9.6$  GeV for  $\gamma p \rightarrow \rho^+ n$ . Notations are the same as Fig. 6. Data of full-square are from Ref. [4] and of empty-square from Ref. [5].

distribution passing over  $-t \approx 0.5$  GeV<sup>2</sup>/c<sup>2</sup>, which is apparent in differential cross sections of  $\rho^+$  at other energy ranges as shown in Fig. 7. Nevertheless, we need more data to confirm such a structure in case of  $\rho^-$  process. Note that our estimate of the contribution of the  $\pi$  exchange to  $d\sigma/dt$  at  $E_\gamma = 9.6$  GeV for the  $\rho^+$  process is similar to that of Ref. [5], but different from that of Ref. [7] at  $E_\gamma = 1.95$  GeV in the case the  $\rho^-$  process.

Fig. 7 displays differential cross sections together with the density matrix elements  $\rho_{\lambda\lambda'}^0$  estimated in the Gottfried-Jackson frame [21, 22] for the unpolarized  $\rho^+$  process. Since the latter observables relate the spin polarization of the final vector meson with that of initial photon in the helicity amplitude, the spin correlations involved in the production mechanism provide a further testing ground for the validity of a model prediction. Within the present framework the density matrix elements are reproduced by the oscillatory behavior of the  $\rho$  exchange due to the canonical phase to agree with data.

In summary, we have investigated photoproduction of charged  $\rho$  for positive and negative based on the Regge model with the  $\gamma\rho\rho$  vertex fully accounting for the magnetic dipole and the electric quadrupole moments. The validity of the Ward identity for the  $\gamma\rho\rho$  vertex is stressed for gauge invariance of the process. With the non-degenerate phase taken for the  $\rho$  exchange from the empirical evidence of the steep decrease in cross sections we show that these processes are dominated by the  $\pi + \rho$  exchanges revealing the nondiffractive feature of the processes as well as the dip structure in the differential cross section and the oscillatory behavior of the density matrix. The role of the  $\rho$ -meson multipoles  $\mu_{\rho^\pm} = \pm 2.01$

and  $Q_{\rho^\pm} = \pm 0.027 \text{ fm}^2$  is investigated in the analysis of the production mechanism to compare to existing data. Measurement of cross sections, in particular, for the  $\gamma p \rightarrow \rho^+ n$  and  $\gamma n \rightarrow \rho^- p$  processes in the resonance region is desirable for further development of the theory for the photoproduction of vector meson.

### ACKNOWLEDGMENTS

We are grateful to Ho-Meoyng Choi for fruitful discussions. This work was supported by the grant NRF-

2013R1A1A2010504 from National Research Foundation (NRF) of Korea.

- 
- [1] R. D. Clark, Phys. Rev. **187**, 1993 (1969).
  - [2] H. M. Choi and C. R. Ji, Phys. Rev. D **70**, 053015 (2004).
  - [3] M. S. Bhagwat and P. Maris, Phys. Rev. C **77**, 025203 (2008).
  - [4] D. P. Barber *et al.*, Z. Phys. C **2**, 1 (1979).
  - [5] J. Abramson *et al.*, Phys. Rev. Lett. **36**, 1432 (1976).
  - [6] H. G. Hilpert *et al.*, Nucl. Phys. B **70**, 93 (1970).
  - [7] P. Benz *et al.*, Nucl. Phys. B **79**, 10 (1974).
  - [8] W. Tang *et al.*, Phys. Rev. C **87**, 065204 (2013).
  - [9] H. Joos and G. Kramer, Z. Phys. **178**, 542 (1964).
  - [10] E. Tomasi-Gustafsson and M. P. Rekalo, Eur. Phys. J. A. **21**, 469, (2004).
  - [11] U. Baur and D. Zeppenfeld, Phys. Rev. Lett. **75**, 1002 (1995)
  - [12] Franz Gross and D. O. Riska, Phys. Rev. C **36**, 1928 (1987).
  - [13] T. D. Lee and C. N. Yang, Phys. Rev. **128**, 885 (1962).
  - [14] S. Brodsky and J. R. Hiller, Phys. Rev. D **46**, 2141 (1992).
  - [15] B. G. Yu, T. K. Choi, and W. Kim, Phys. Rev. C **83**, 025208 (2011).
  - [16] S. Ishida, K. Yamada, and M. Oda, Phys. Rev. D **40**, 1497 (1989).
  - [17] G. Erkol, R. G. E. Timmermans, M. Oka, Th. A. Rijken, Phys. Rev. C **73**, 044009 (2006).
  - [18] M. Clark and A. Donnachie, Nuclear Materials B **125**, 493 (1977).
  - [19] M. Guidal, J.-M. Lajet, and M. Vanderhaeghen, Nucl. Phys. A **627**, 645 (1997).
  - [20] Harry J. Lipkin, *Lie Groups for Pedestrians*, North-Holland, 1965, p147.
  - [21] K. Schilling, P. Seyboth, and G. Wolf, Nucl. Phys. B **15**, 397 (1970).
  - [22] Qiang Zhao, J. S. Al-Khalili, and P. L. Cole, Phys. Rev. C **71**, 054004 (2005).